Development of Filled-Skutterudite Based Thermopile for High Temperature Sensors for Space and Terrestrial Applications

Kevin L. Smith[1], Billy Chun-Yip Li[1], Samad Firdosy[1], Sutine Sujittosakul[1], Michael Errico[1], George Nakatsukasa[1], Jean-Pierre Fleurial[1], and Richard Ewell[1]

[1]Jet Propulsion Laboratory/Caltech, MS 277-207
4800 Oak Grove Drive, Pasadena CA, 91107
818-394-9443, Kevin.L.Smith@jpl.nasa.gov

The Thermal Energy Conversion Technologies Group at the Jet Propulsion Laboratory has been pursuing the development of thermopiles capable of higher temperature operation in support of terrestrial and space sensing applications in extreme environments. The next-generation sensor technology would rely on filled skutterudite (SKD) compounds, the same materials currently being considered for use in the enhanced Multi-Mission Radioisotope Thermoelectric Generator (eMMRTG). We report on the design, development and fabrication of SKD-based prototype thermopile devices. The beginning-of-life (BOL) experimental and predicted performance of the SKD-based prototype thermopile in terms of electrical resistance, output voltage, current, power output and efficiency in the 423 to 723 K operating temperature range is reported and discussed .

Nomenclature

eMMRTG	=	Enhanced Multi-Mission Radioisotope Thermoelectric Generator
α	=	Seebeck coefficient (μV/K)
η_{max}	=	Maximum couple thermal-to-electric conversion efficiency
λ	=	Thermal conductivity (W/m-K)
T_H	=	Hot junction temperature
T_C	=	Cold junction temperature
T_{ave}	=	Average couple temperature
Z	=	Thermoelectric figure of merit
CTE	=	Coefficient of thermal expansion

I. Introduction

Thermoelectric power sources have been successfully used by NASA for space science and exploration missions for over 50 years. These robust systems, producing 10's to 100's of watts, typically use converters composed of hundreds of discrete couples that are conductively or radiatively coupled to a high temperature heat source, and are interconnected on the cold side in a series-parallel "laddering" pattern to achieve high redundancy and eliminate single point failures. Such couples typically produce open circuit voltage on the order of a tenth of a volt per couple. For "low power" converter and thermal sensor designs, the use of discrete couples becomes impractical because achieving reasonable output voltages (> 5V) requires integrating a large number of couples with high aspect ratio. The best approach for practical and efficient thermal and mechanical integration with the heat source and heat rejection system components is to assemble these high aspect ratio couples into robust TE module structures, or thermopiles. Current state-of-practice thermopile technology is based on Bi_2Te_3 alloys that is limited to hot side operating temperatures close to 500 K.[1] More recently there has been renewed interest in developing thermopile technology capable of higher temperature operation in support of low power and sensing applications in extreme terrestrial and space[2] environments. New thermoelectric couple technology based on filled skutterudite (SKD) compounds is currently being considered for application to automotive waste heat recovery[3] and potential infusion

into an enhanced Multi-Mission Radioisotope Thermoelectric Generator (eMMRTG) for future space science and exploration missions[4]. This technology is also suitable for use in thermopile devices capable of operating up to 875K and we report on the design, development and initial performance testing of SKD-based thermopiles.

II. Experimental Procedures

A. Preparation of p-Type and n-Type Skutterudite Leg Components

Both p-type and n-type Skuterudite (SKD) powder were synthesized via mechanical alloying at JPL in ~ 100 g batches. The nominal chemical composition of the p-type skutterudite was $Ce_{0.9}Fe_{3.5}Co_{0.5}Sb_{12}$ and n-type skutterudite was $Ba_{0.05}Yb_{0.15}Co_4Sb_{12}$. A quality analysis of each newly synthesized batch of SKD powder was performed by measuring electrical resistivity, Seebeck, and thermal conductivity before moving to the next step in production. Once the powder passed the QA process it was then inserted into a graphite die, pressed into a green cylindrical puck at room temperature under an inert environment, and hot pressed in argon/vacuum with metallization foils bonded in-situ. Fig. 1a shows an example of a pre-metallized SKD puck. Both p- and n-SKD pucks were 32 mm in diameter and 10.2 mm in thickness, including the metallization layers. The thin metallization layers allow leg components to be brazed or soldered to a metal interconnect and also act as a diffusion barrier to prevent Sb in the material from reacting with the metal interconnects. Pucks were inspected for cracking, inclusions, chipping, and foil delamination optically. Densities were measured by weighing the pucks in air and measuring volume geometrically. The hot press process produced metallized p- and n-SKD pucks with densities typically 99% or above of the theoretical value. The pucks were then diced into legs with a cross section of 1 mm by 1 mm and a length of 10.2 mm. The pucks produced were robust enough to withstand the stresses involved in dicing and lapping individual leg components, shown in Fig. 1b.

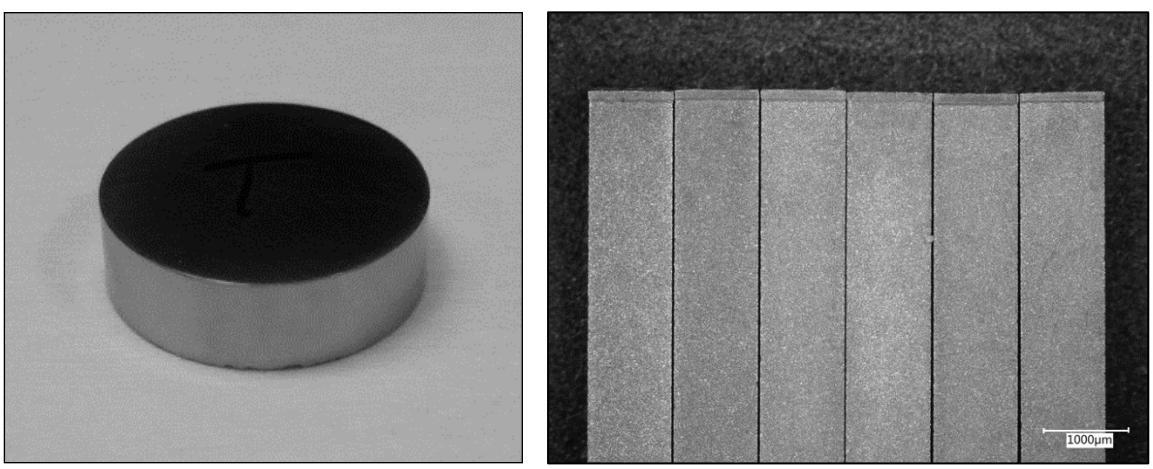

(a) **(b)**

Figure 1. (a) Pre-metallized Skutterudite puck, 32 mm in diameter and 10.2 mm tall (b) A zoomed image of diced SKD legs. Each leg shown was 1 mm by 1 mm in cross section and 10.2 mm in length.

B. Thermopile Design and Fabrication Techniques

Thermoelectric leg components must be connected in p-type and n-type arrangements to form a couple. Each leg component must also be connected electrically in series and thermally in parallel within the thermopile, with interconnect pads that are electrically isolated from each other. On a couple to couple level, series or parallel arrangements can be designed. The thermopiles described here were designed such that all of the couples were connected electrically in series in order to generate as high a voltage as possible. Fig. 2 shows a top view of the thermopile end plates used in a 4x5 leg arrangement (20 legs, 10 couples). A thin sheet of alumina was used to support the metal interconnect pads and the overall thermopile design was guided by a detailed finite element analysis to address mechanical integration and operation challenges. The alumina sheet was initially fully metallized, then a grid was subsequently cut to form the electrically isolated pads. Grid supports were designed to support and align the legs during the fabrication process. A custom fixture was designed to hold the thermopile components during the thermopile assembly and bonding process. The dimensions of the thermopiles were 7.45 mm x 12 mm and 12.5 mm tall. Smaller thermopiles with 3 couples (6 legs) shown in Fig. 3a were fabricated to develop the fabrication process

and for rapid performance evaluations. Larger thermopiles with 10 couples (20 legs) shown in Fig. 3b and Fig. 4 were then fabricated for full performance evaluation. None of the thermopiles were encapsulated with thermal insulation, but an aerogel encapsulation process is planned for future work.

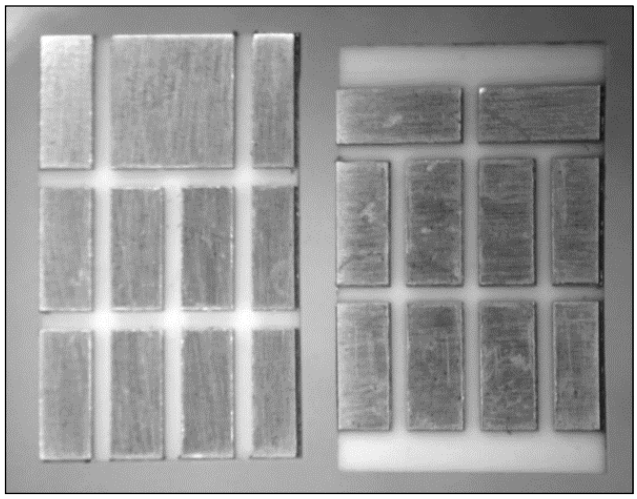

Figure 2. Alumina endplates with metallic interconnect pads.

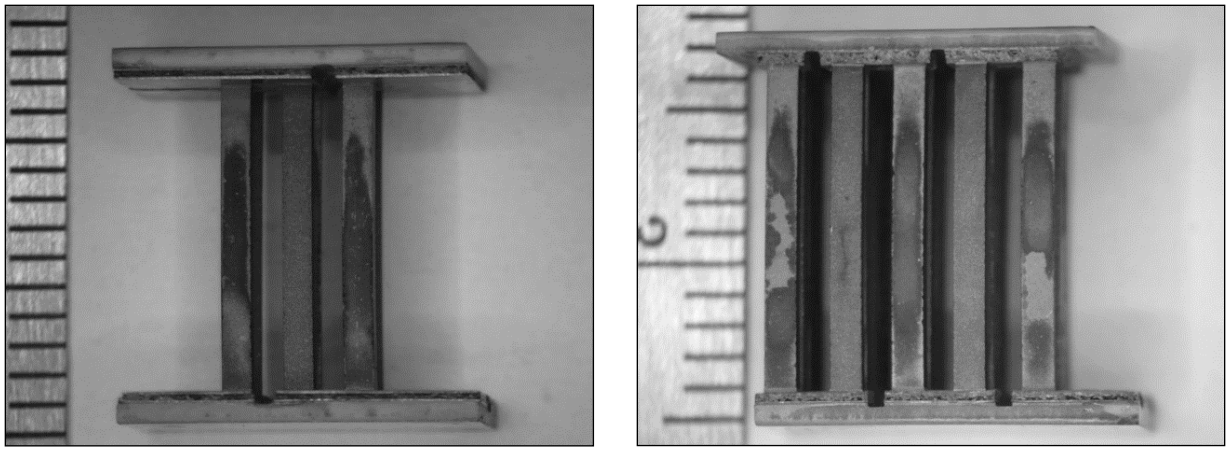

(a) **(b)**

Figure 3. (a) Side view of a 2x3 thermopile (3 couples), 1div = 1 mm (b) Side view of a 4x5 thermopile (10 couples), 1 div = 1 mm.

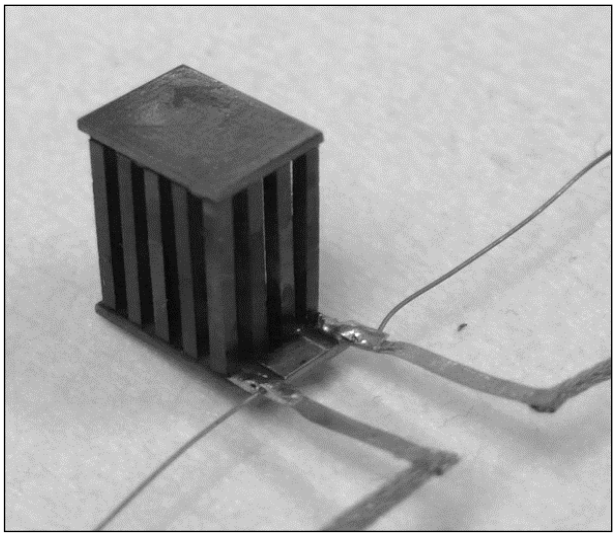

Figure 4. Isometric view of a 4x5 thermopile (10 couples) after wiring.

C. Performance Test Set Up

A fixture was designed and fabricated to secure the thermopile via spring load and to hold the heaters used to pass heat though the device. The hot side and cold side temperatures of the device were controlled and heat was sunk though a water cooled Cu plate. No thermal insulation was used to insulate the thermopiles and all experiments were performed in a high vacuum environment. Temperatures were measured by inserting thermocouples into copper plates sandwiched above and below the thermopile. Fig. 5 shows a side view of a 2x3 3-couple thermopile in the performance test fixture. Thermocouples were inserted in the holes shown in Fig. 5 and temperature was controlled from the Cu plate holes closest to the top and bottom alumina endplates. The thermopile was sandwiched between the heat source and sink and approximately 1.4 kg of spring load force was applied to the thermopiles during testing. Grafoil was used as a thermal contact interface on the hot and cold side of the device. Temperature drops across the grafoil contact interface were measured and taken into account. A LabVIEW program was developed to control the current sweep and record temperature and voltage data. Electric current (DC) was passed through the device, held for 0.5 second, voltage and temperatures were recorded, then the current would step to the next magnitude and repeat the step-measure-step process. This set up provided a precisely controlled current sweep at a relatively low current. Temperature fluctuations caused by the Peltier effect due to varying the current were minimal.

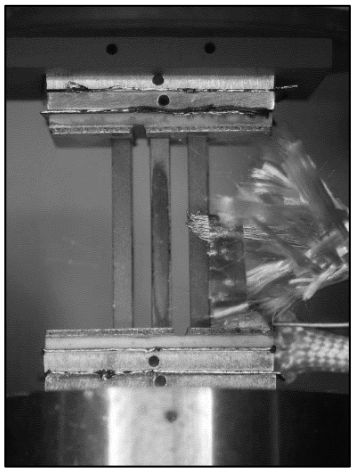

Figure 5. Image showing a 2x3 thermopile spring loaded in the performance test fixture. Thermocouples were inserted in the holes shown.

III. Results and Discussion

Beginning of life performance of each type of thermopile was evaluated at JPL. The smaller 2x3 thermopile was tested under a constant cold side temperature while the hot side was adjusted. The 4x5 thermopile was tested while in contact with a heat source held at 824 K and a heat sink held at 424 K. The exact temperatures at the SKD junction was difficult to ascertain and can vary depending on the type of thermal interface used to contact the heat source and sink. Voltages were generated due to the temperature difference across the legs as defined by the thermoelectric open circuit voltage equation shown below:

$$V_{oc} = n\int_{T_C}^{T_H} \alpha_p(T)dT - n\int_{T_C}^{T_H} \alpha_n(T)dT \tag{1}$$

Where n is the number of p or n leg components, T_H and T_C are the hot and cold junction temperature of the SKD leg, and alpha is the temperature dependent Seebeck coefficient of the p or n legs. An integration is required due to the temperature gradient imposed upon the legs. The n-type SKD will produce a negative potential at the cold end and the p-type will produce a positive potential at the cold end; therefore, the V_{oc} of p and n components will add together. Measured V_{oc} values for the 2x3 thermopile at various hot side temperatures with a constant cold side temperature are shown in Fig. 6a at the y-intercept. The measured voltage shown in Fig. 6a was linear as a function of current and is defined in this case by:

$$V = V_{oc} - IR_{int} \tag{2}$$

Where V_{oc} is the open circuit voltage defined by Eq. 1, I is the current magnitude, and R_{int} is the internal resistance of the thermopile. R_{int} is the negative slope of the linear I-V plots shown in Fig. 6a and includes the resistance from the TE material and the electrical contact resistances at the hot side and cold side junctions of the TE material, all of which vary with temperature.

The maximum power and V_{oc} achieved by the 2x3 thermopile in this experiment was 35 mW and 263 mV respectively with the heat source temperature at the hot side of the device set at 724 K and the cold side set point held at 424 K.

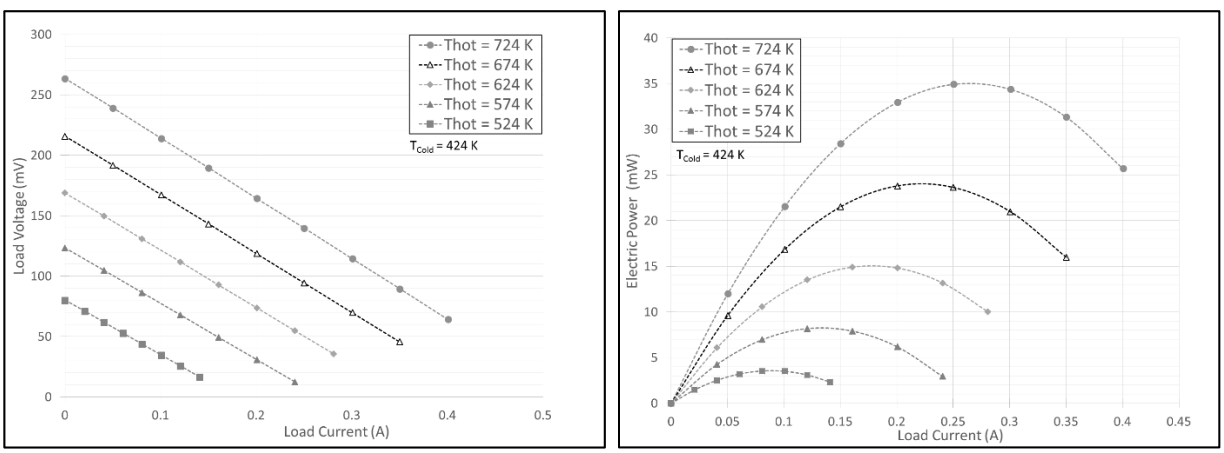

(a) **(b)**

Figure 6. Measured performance data of a 2x3 thermopile under a constant cold side temperature of 424 K while varying the hot side temperature in increments of 50 K from 524 K to 724 K. Figure (a) Shows the 2x3 thermopile voltage as a function of current. The slope of the I-V curves equate to the device internal resistance. Figure (b) Shows the electric power as a function of current.

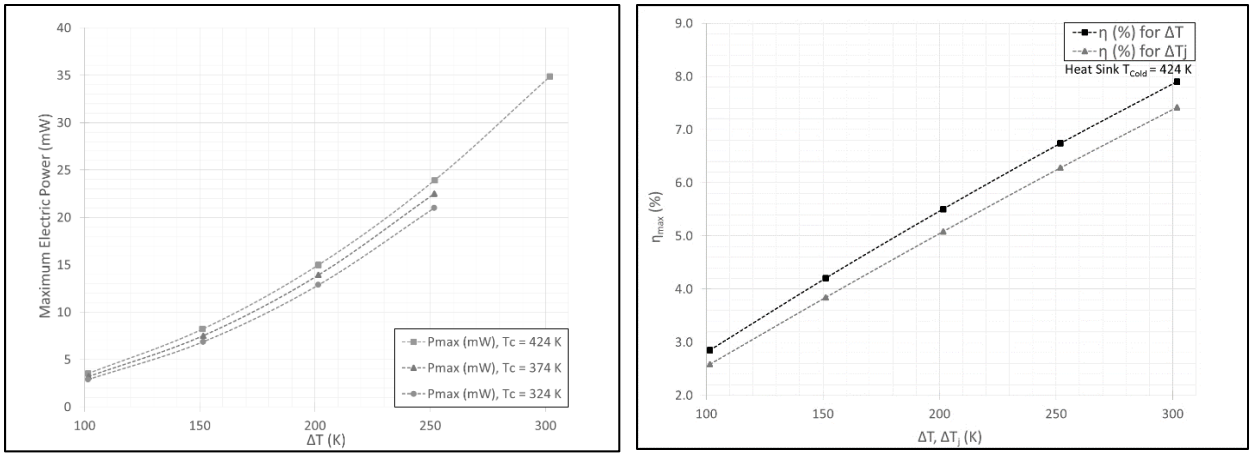

(a) **(b)**

Figure 7. (a) Measured maximum power data of a 2x3 thermopile under constant cold side temperatures while varying the hot side temperature in increments of 50 K. (b) Measured % efficiency of a 2X3 thermopile with the cold side held at 424 K and the hot side varied by 50 K.

Fig. 7a demonstrates that the power of the device will increase as the temperature difference across the legs increases, but the maximum power also increases when the magnitude of T_H and T_C increase at constant ΔT. The set point temperatures of the hot and cold source and the actual SKD junction temperatures can vary based on thermal contact between the heat source and the thermopile. The thermal contact resistance can vary depending on pressure, interface material, temperature, etc. as discussed in Ref. 3 and is a big factor in the efficiency of the thermopile. Another big factor is the temperature drop across the ceramic plates and interface pads. Fig. 7b shows plots of maximum couple thermal-to-electric conversion efficiency (η_{max}) in terms of percentage as a function of the temperature drop across heat sink to heat source (ΔT) and the estimated SKD junction temperatures (ΔT_j).

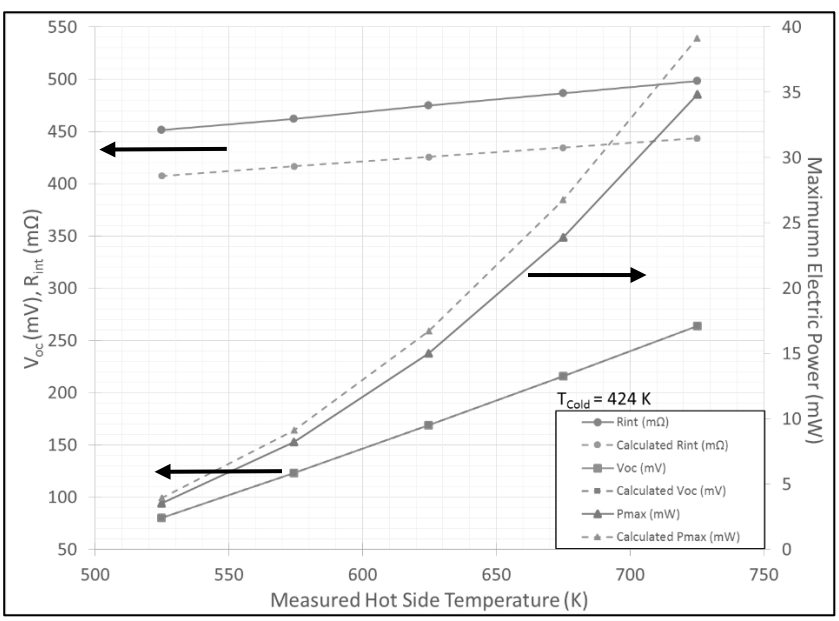

Figure 8. Measured vs. calculated data of a 2X3 thermopile under constant cold side temperature set at 424 K while varying the hot side set point temperature in increments of 50 K from 524 K to 724 K.

Fig. 8 shows calculated values of R_{int} and maximum power in the dotted lines verses measured values in solid lines. The calculated resistance and power required junction temperature predictions that were obtained using Eq. 1 by iterating the temperatures until the calculated V_{oc} value matched the measured value. This is why the measured and calculated lines in Fig. 8 overlay each other. Results show that the measured thermopile internal resistance is

consistently about 12 to 13% higher than predicted, leading to a similar drop in maximum power output. The discrepancy is mostly attributed to the higher electrical resistance at the hot side SKD leg-metal interconnect interfaces.

A 4x5 thermopile was also tested under the same conditions as the 2x3 except a higher hot side set point temperature at T_h = 824 K was used, with cold side set point T_c = 424 K. As shown in Fig. 9, max power was 0.17 W and V_{oc} was 1.19 V. This was also in reasonably good agreement with initial predictions.

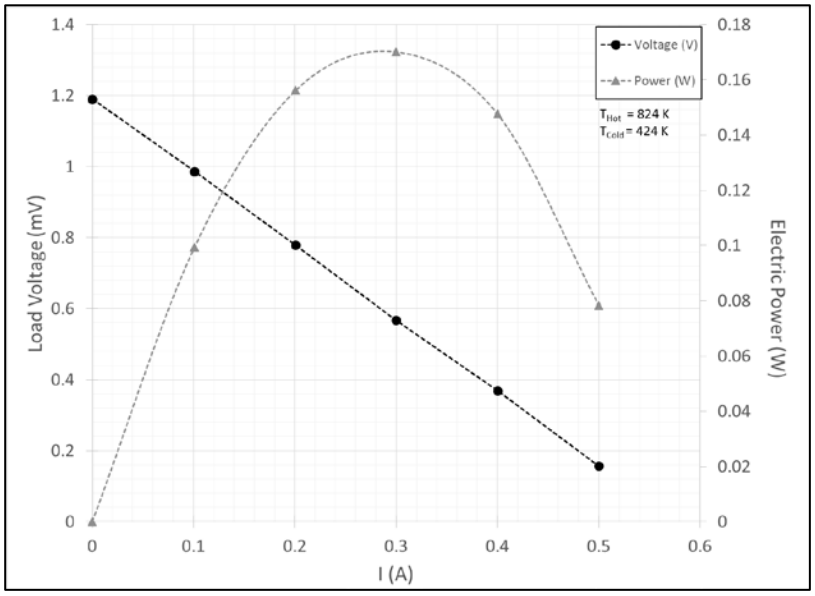

Figure 9. Measured data of a 4x5 thermopile (10 couples) under constant cold side temperature set at T_c = 424 K and a constant hot side at T_h = 824 K.

Although these results are promising, additional work to improve the 4x5 thermopile fabrication process continues. Further study of the temperature dependence of the electrical contact resistance is also underway.

IV. Conclusion

A proof of concept Skuterudite mini-thermopile prototype has been developed at JPL in 3 couple and 10 couple device configurations that can withstand higher temperatures (~ 875 K versus 500 K for Bi_2Te_3-based state-of-practice technology) and could potentially be used for a number of extreme environment applications. Techniques and materials have been developed to dice high aspect ratio pre-metallized skutterudite leg components. A custom process for fabricating and performance testing the device has also been developed. Future work includes a focus on testing the thermopiles for longer time durations with hopes to understand and predict performance vs. lifetime.

Acknowledgments

The work described in this proceeding was carried out at the Jet Propulsion Laboratory/ California Institute of Technology, under contract with the National Aeronautics and Space Administration. The authors would like to thank Dr. Chen-Kuo Huang for Skutterudite powder synthesis.

References

[1]Snyder, G. J., et al , "Testing of Milliwatt Power Source Components," *21st International Conference on Thermoelectrics*, 2002, pp. 463, 470.

[2]Pauken, M., Smith, K., Fleurial, J.-P., and Smrekar, S., "Venus Heat Flux Sensor Instrument Development", Thirteenth meeting of the Venus Exploration and Analysis Group (VEXAG), October 27-29 (2015).

[3]Salvador, J. R., et al, "Conversion efficiency of skutterudite-based thermoelectric modules," *Phys. Chem. Chem. Phys.*, Vol. 16, No. 24, 28 Jun. 2014, pp. 12510-20.

[4]Holgate, T.C., et al. « « J. of Electronic Materials, June 2015, Vol. 44, Issue 6, pp 1814–1821.